Development of a 488-nm Blue Laser for Biomedical Analyzers

*by Takeshi Takagi *, Hiroshi Matsuura *, Akira Fujisaki * and Tomoya Kato *2*

ABSTRACT The authors have developed a 488-nm blue laser by combining a 976-nm semiconductor laser Furukawa Electric has long fostered in the optical communications field with a wavelength conversion device based on periodically poled lithium niobate (PPLN). Because of its simple device configuration whereby the semiconductor laser for optical communications —where long-term reliability up to 20 years is required— is directly coupled with the wavelength conversion device, the laser has a long service life, compact size, low cost, and low power consumption. Moreover, by optimizing the spectrum of fundamental lightwave and by providing a feedback circuit in which a fraction of the output light is monitored for control use, the laser has achieved both high output stability and low noise that were unattainable for conventional argon lasers and diode pumped solid state (DPSS) lasers. The obtained performance, i.e. output power ≥20 mW, output power stability <2 %, peak-to-peak noise < 1 %, and rms noise < 0.25 %, was confirmed to meet the characteristics required for light sources for biomedical analyzers. In the future strong demand is expected as a light source for bioinstrumentation.

1. INTRODUCTION

Recently, with the aging of society and the advancement of medical technologies such as gene-analysis, the bio-analysis equipment industry continues to expand. And flow cytometer (FCM) is one of these equipment for cell-analysis.

FCM illuminates cells with a laser beam to analyze and sort the cells based on the scattered light and fluorescence, using a 488-nm blue laser as the light source for exciting the fluorescence. Although argon laser constituted the mainstream of 488-nm laser light sources through the ages, it had problems specific to gas lasers such as short service life, large size, noise, vibration, high power consumption, heat generation, and need for regular maintenance, so that there has been a strong need for a solid state blue laser for bioinstrumentation.

DPSS laser has been developed and marketed in recent years, but the laser has not solved the issue of heat generation nor the difficulty in cost reduction due to its structure.

Furukawa Electric has an impressive track record in the field of optical telecommunications, in the manufacture of 980-nm pumping lasers for optical communications and optical modules, and taking advantage of these technologies, the Company has lately developed a 488-nm blue laser to replace gas lasers. The new laser uses a 976-nm semiconductor laser shown in Figure 1 for fundamental lightwave generation and a PPLN device for second harmonic generation (SHG), thereby outperforming both argon laser and DPSS laser. The developmental work of this blue laser light source will be described in this paper.

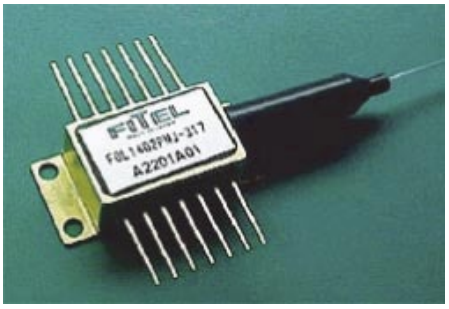

Figure 1 976-nm semiconductor laser.

2. CONFIGURATION OF 488-NM BLUE LASER

Figure 2 shows the configuration of the blue laser developed here. A 976-nm semiconductor laser is employed as fundamental lightwave generator, and after wavelength stabilization using fiber Bragg grating (FBG), the source light is directly coupled to a SHG wavelength conversion device of planar waveguide type.

Because, in single-longitudinal-mode operation, the 976-nm semiconductor laser is subject to mode hopping due to fluctuations in the driving current, the laser is provided with an anti-mode hopping structure of multi-longitudinal-mode, and moreover, the reflection characteristics

* FITEL-Photonics Lab., R&D Div.
*2 Corporate Strategy Planning Dept.

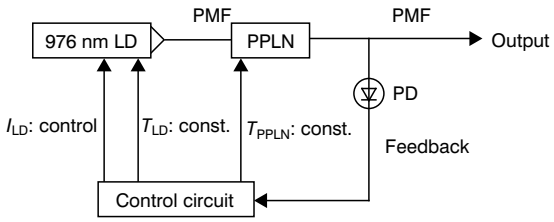

Figure 2 Configuration of 488-nm blue laser.

of the FBG are optimized to stabilize the wavelength. In this way second harmonic generation of high efficiency and stability has been achieved despite the use of PPLN which is known for its sensitivity to wavelength changes. Moreover, since PPLN is also sensitive to temperature changes, the device temperature is controlled within a range of 0.5°C using a Peltier cooler.

Each device is optically connected using a polarization maintaining fiber (PMF) for specific use. In particular, the asymmetrical beam output from the PPLN waveguide is ideally shaped into a symmetrical beam by the use of PMF.

In addition, to stabilize the optical output power, the blue light output from the PPLN waveguide, monitored by a photo diode, is used to control the output power suppressing its fluctuation.

3. DEVELOPMENT TARGETS

Table 1 shows the target specifications of this development. The specifications were established, making reference to those of argon lasers and DPSS lasers used in the existing biomedical applications, to satisfy the requirements for bio-analysis light sources.

4. SIMULATION AND FUNDAMENTAL EXPERIMENTS

In SHG that takes advantage of non-linear optical effects, both conversion efficiency and output power stability become important. Theoretically, high conversion efficiency could be obtained by narrowing the line width of fundamental lightwave thereby increasing the peak power, but this would result in unstable output power due to fluctuations in the spectrum of fundamental lightwave. Because the allowable range of wavelength conversion device is rather narrow, fluctuations in the spectrum of fundamental lightwave significantly influence the SHG output power. Moreover, in the case of 976-nm semiconductor laser, it is technologically difficult to completely stabilize the spectrum under the influence of possible mode hopping. Accordingly, we broadened the spectrum of the 976-nm semiconductor laser thereby optimizing it to an extent such that a conversion efficiency resulting in an output power of not less than 20 mW be obtained and that the influence of mode hopping of the laser on the SHG output power be minimized. Figure 3 shows a typical spectrum of the fundamental lightwave thus determined.

Table 1 Target specifications.

Parameter	Unit	HPU50204 spec.
Power	mW	≥20
Wavelength	nm	488±2
Spatial mode	M^2	≤1.2
Beam asymmetry	—	≤1.15
Beam diameter (1/e²)	mm	0.7±0.15
Beam divergence	mrad	≤1.25
Pointing stability	μrad	≤10
Noise (20 Hz~2 MHz, rms)	%	≤0.25
Noise (20 Hz~20 kHz, p-p)	%	≤1
Long term power stability (2 h, ±3°C)	%	≤2
Warm up time	min	≤5
Polarization ratio	dB	≤16
Operating temperature	°C	10 ~ 40

In the case of a light source with a fundamental lightwave of broad line width as shown in Figure 3, it is known that the sum frequency generation (SFG) theory works better than the SHG theory in calculating the secondary wave in good agreement with experimental results.

Let us, in accordance with the SFG theory, divide the incident lightwave into N fractions according to the wavelength and assume that a lightwave with an arbitrary wavelength λ_i couples with all the lightwaves with a wavelength λ_j in an independent manner to generate a lightwave with a wavelength λ_{ij} such that

$$\frac{1}{\lambda_{ij}} = \frac{1}{\lambda_i} + \frac{1}{\lambda_j} \quad (1).$$

Writing the phase mismatch condition as

$$\Delta k = k_{ij} - k_i - k_j - k_G \quad (2)$$

where: k_G is the coefficient related with the poling reversal frequency of PPLN,

the SFG intensity can be obtained by solving the electric field equations as

$$I_s(\zeta)^2 = \frac{1}{N}\sum_{i,j-1}^{N} \frac{8\pi\omega_{ij}^2 W}{c^2 k_{ij}} u_{ija}^2 sn^2(|u_{ijb}|\zeta,\gamma) \quad (3).$$

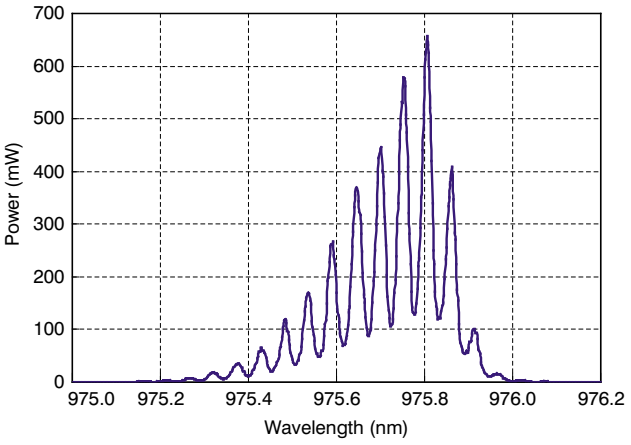

Figure 3 Typical spectrum of 976-nm fundamental lightwave.

Here,

$$u_i = \left(\frac{c^2 k_i}{8\pi\omega_i^2 W 10^9}\right)^{1/2} E(\lambda_i)$$

$$u_j = \left(\frac{c^2 k_j}{8\pi\omega_j^2 W 10^9}\right)^{1/2} E(\lambda_j) \quad (4)$$

$$u_{ij} = \left(\frac{c^2 k_{ij}}{8\pi\omega_{ij}^2 W 10^9}\right)^{1/2} E(\lambda_{ij})$$

$$\zeta = K\left(\frac{8\pi W}{c^2}\right)^{1/2}\left[\frac{\omega_i^2\omega_j^2\omega_{ij}^2}{k_i k_j k_{ij}}\right]^{1/2} z$$

and

$$W = \frac{c^2}{8\pi\cdot 10^9}\left[\frac{k_i}{\omega_i}E(\lambda_i)^2 + \frac{k_j}{\omega_j}E(\lambda_j)^2 + \frac{k_{ij}}{\omega_{ij}}E(\lambda_{ij})^2\right] \quad (5).$$

Equation (5) defines the lightwave propagation within the waveguide.

In effect, however, all fundamental lightwaves interact with each other, which should be taken into account in the deriving process of SFG. Accordingly, two variables $f(N)$ and α are introduced here as

$$W' = f(N)\cdot W = f(N)\frac{c^2}{8\pi\cdot 10^9}\left[\frac{k_i}{\omega_i}E(\lambda_i)^2 + \frac{k_j}{\omega_j}E(\lambda_j)^2 + \frac{k_{ij}}{\omega_{ij}}E(\lambda_{ij})^2\right] \quad (6)$$

Nomenclature

c	velocity of light
E	electric field
f	interaction function
I	intensity
k	phase
K	effective nonlinear function of PPLN
N	wavelength fraction
sn	Jacobi elliptic functions
u	substitution variable
W	power flow per unit area parallel to the propagation direction
z	direction of propagation

Greek letters

α	interaction coefficient
ζ	substitution variable
λ	wavelength
ω	angular frequency

Subscripts

i	fundamental index
j	fundamental index
ij	SFG index
G	PPLN period
S	SFG

and

$$\Delta k' = \Delta k^{\alpha} = (k_{ij} - k_i - k_j - k_G)^{\alpha} \quad (7)$$

to achieve good agreement between the calculated and experimental results.

Figure 4 shows comparisons of spectrum between the calculated and experimental results. When the controlled temperature for the PPLN is changed, the phase mismatch condition shifts resulting in a change in the secondary harmonic spectrum. This, in addition to good agreement between the calculated and experimental results, can clearly be seen in Figure 4.

Figure 5 plots the conversion efficiency when the spectrum shown in Figure 3 is used as a fundamental lightwave. It has been confirmed that a conversion efficiency of not less than 10 % over the fundamental lightwave, i.e. 40 mW or higher in terms of 488-nm output power, has been achieved amply allowing the manufacture of light sources with an output power of not less than 20 mW.

5. CHARACTERISTICS EVALUATION

Figure 6 shows the appearance of the blue laser (product code: HPU50204) developed here. The product has

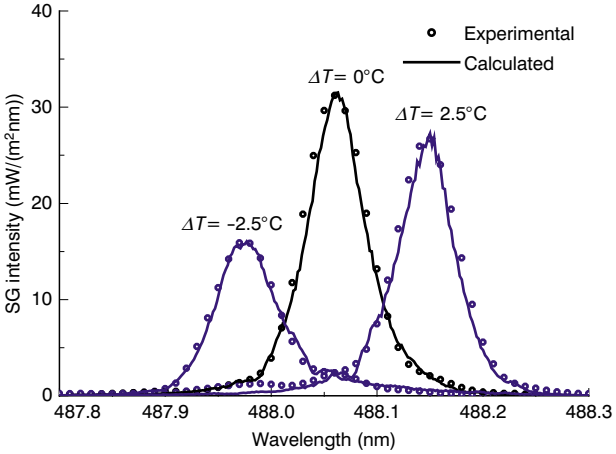

Figure 4 Comparisons of spectrum between the calculated and experimental results.

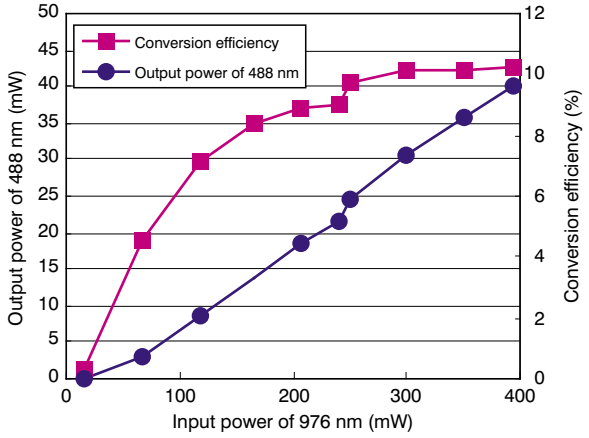

Figure 5 Conversion efficiency and output power using the SFG theory.

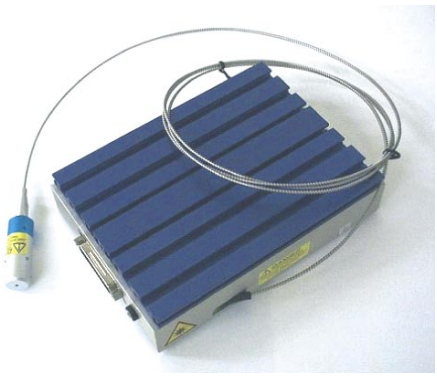

Figure 6 Appearance of HPU50204, 488-nm SHG blue laser.

achieved a compact size of 177L × 127W × 40.8H and a low power consumption of 18 W. The use of a pigtail fiber for output termination allows easy handling, and it can be adapted to application of connector or collimator.

5.1 Noise Characteristics

The output laser light was photoelectrically converted using a photo diode, and after *I-V* conversion, fluctuation components (p-p, and rms) at each frequency band was measured using an oscilloscope. Table 2 shows the results.

Whereas noise characteristics are important for light sources for biomedical analysis, the laser has achieved the target specifications of p-p < 1 % and rms < 0.25 % with a sufficient margin.

5.2 Output Power Stability

Output power stability was evaluated and the results are shown in Figure 7. The stability was 0.24 %, amply satisfying the specification of less than 2 %. In the continuous operation for two weeks the stability was 1.37 %, a satisfactory value.

5.3 Wavelength Stability

The stability of output spectrum was measured using a spectrum analyzer (ANDO AQ6315). The results are shown in Figure 8. Both the center wavelength and FWHM are seen to be stable, indicating that the spectrum of fundamental lightwave is stabilized and that the temperature of PPLN is stably controlled.

Table 2 Results of noise characteristics measurement.

Optical power (mW)	Filter (kHz)	Noise (%)	
		p-p	rms
20	20000	0.124	0.027
	1280	0.144	0.032
	320	0.210	0.039
	160	0.185	0.035
	20	0.210	0.034
	10	0.210	0.036

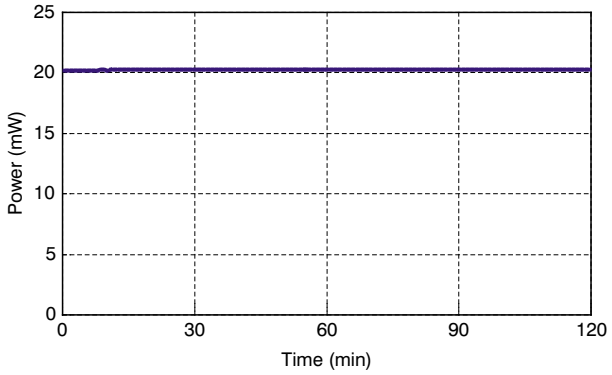

(a) For 2 hours

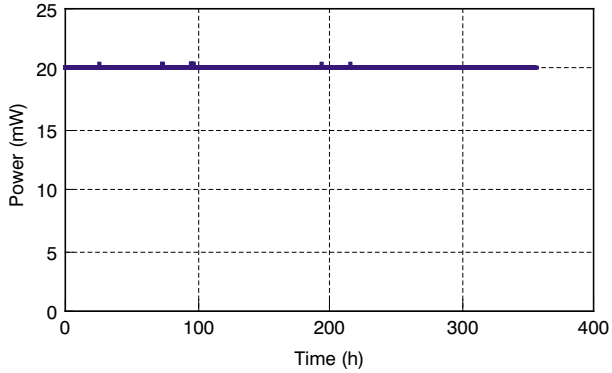

(b) For 2 weeks

Figure 7 Output power stability.

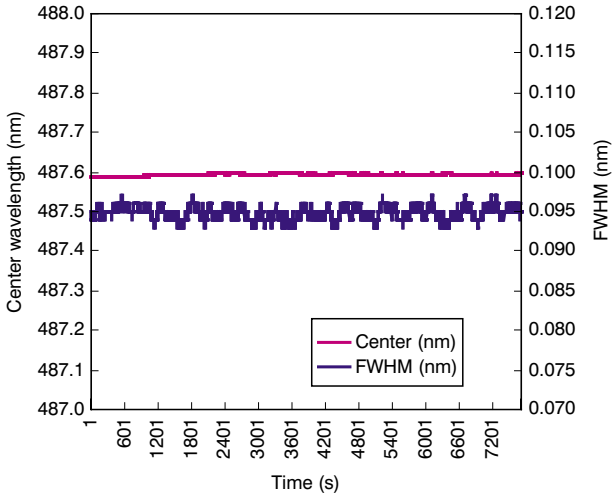

Figure 8 Results of wavelength stability measurement.

5.4 Temperature Characteristics

Figure 9 shows the results of temperature characteristics measurement. In the measurement, temperature cycle of 10°C~40°C was applied with a temperature gradient of 6°C/h, severer than the specification of 6°C/2h. The output power levels at 10°C and 40°C were 20.38 mW and 19.85 mW respectively, indicating a fluctuation margin of 2.6 %, a satisfactory stability in the service environment.

5.5 Beam Property

The output beam of the blue laser developed here was collimated using a f3.85 lens, and the beam parameters

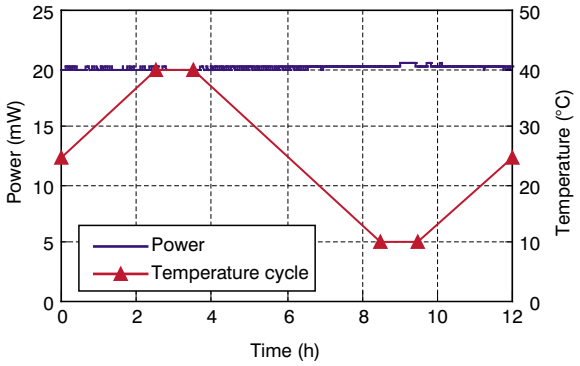

Figure 9 Results of temperature characteristics measurement.

were measured using a beam profiler. The results are shown in Table 3 and Figure 10. It can be seen that an ideal beam shape of $M^2 < 1.2$ has been obtained, and that both the beam width and beam divergence meet the target specification.

In this connection, because the output of the blue laser developed here is terminated with a pigtail fiber, any beam width is available by selecting an appropriate lens.

5.6 Beam Pointing Stability

Figure 11 shows the evaluation system for beam pointing stability. While beam pointing stability poses a problem in argon lasers because their beam position fluctuates due to heat generation and vibration, the blue laser developed here has its pigtail fiber termination collimated, so that there is no problems whatever in terms of heat generation and vibration of laser head. The measurement result

Table 3 Results of beam parameter measurement.

Parameter		X	Y	R
Spatial mode	(M^2)	1.049	1.112	1.081
$2W_o$	(mm)	0.5722	0.5988	0.5859
$2W_e$	(mm)	1.0015	1.0512	1.0266
Z_o	(m)	−0.72	−0.7471	−0.7337
Z_r	(mm)	0.5012	0.5178	0.5099
Divergence	(mrad)	1.142	1.156	1.149
Astigmatism $(Z_{oy}/Z_{ox})/Z_{rr}$	(%)		5.31	
Waist asymmetry $(2W_{oy}/2W_{ox})$			1.0465	
Divergence asymmetry (θ_y/θ_x)			1.0129	

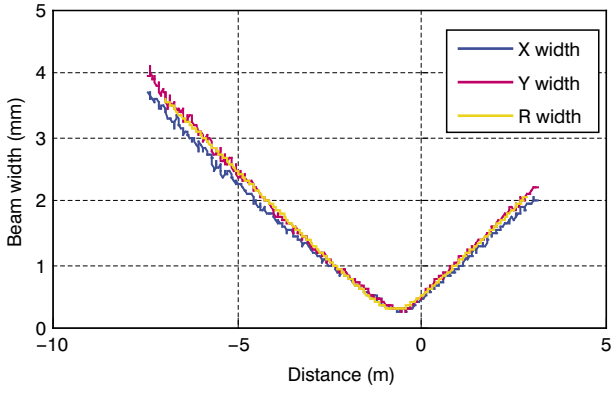

Figure 10 Beam width in external propagation.

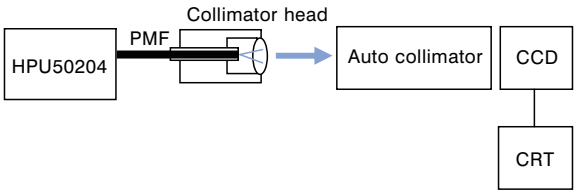

Figure 11 Measurement system for beam pointing stability.

shows satisfactory stability below the detection limit of 0.0024 mrad.

6. LONG-TERM RELIABILITY

The long-term reliability is now being evaluated under continuous operation. As of July XX, 2005, there is no problems after Y months have elapsed. A long service life is reasonably anticipated since a semiconductor laser for telecommunications is used for fundamental lightwave generation.

7. CONCLUSION

The authors have developed the 488-nm blue laser by combining the 976-nm semiconductor laser with the wavelength conversion device. Due to its simple device configuration the laser has a long service life, compact size, low cost, and low power consumption. In the future strong demand is expected as a light source for bioinstrumentation in place of argon laser and DPSS laser.

REFERENCES

1) M. M. Fejer, G. A. Magel, D. H. Jundt and R. L. Byer: J. Photo Elect. 28 (1992) 2631.
2) J. A. Amstrong, N. Bloembergen, J. Ducuing and P. S. Pershan: Phys. Rev. 127 (1962) 1918.
3) A.Yariv: Optical Electronics (Saunders College Publisher, City of publication, 1991) 4th ed., Chap. 8, p. 258.